© 1999 Nature America Inc. • http://genetics.nature.com

# Irs-2 coordinates Igf-1 receptor-mediated β-cell development and peripheral insulin signalling

Dominic J. Withers[1,2*], Deborah J. Burks[1*], Heather H. Towery[1], Shari L. Altamuro[1], Carrie L. Flint[1] & Morris F. White[1]

*These authors contributed equally to this work.

**Insulin receptor substrates (Irs proteins) mediate the pleiotropic effects of insulin and Igf-1 (insulin-like growth factor-1), including regulation of glucose homeostasis and cell growth and survival. We intercrossed mice heterozygous for two null alleles (*Irs1*$^{+/-}$ and *Irs2*$^{+/-}$) and investigated growth and glucose metabolism in mice with viable genotypes. Our experiments revealed that Irs-1 and Irs-2 are critical for embryonic and post-natal growth, with Irs-1 having the predominant role. By contrast, both Irs-1 and Irs-2 function in peripheral carbohydrate metabolism, but Irs-2 has the major role in β-cell development and compensation for peripheral insulin resistance. To establish a role for the Igf-1 receptor in β-cells, we intercrossed mice heterozygous for null alleles of *Igf1r* and *Irs2*. Our results reveal that Igf-1 receptors promote β-cell development and survival through the Irs-2 signalling pathway. Thus, Irs-2 integrates the effects of insulin in peripheral target tissues with Igf-1 in pancreatic β-cells to maintain glucose homeostasis.**

© 1999 Nature America Inc. • http://genetics.nature.com

## Introduction

Insulin and Igf-1 bind to distinct cell-surface receptor tyrosine kinases that regulate a variety of signalling pathways controlling metabolism, growth and survival[1–6]. Mice without *Igf1r* have retarded growth and die at birth, whereas mice lacking the insulin receptor display normal intrauterine growth but die within 72 hours due to severe hyperglycaemia and ketoacidosis with hyperinsulinaemia[7,8]. Mice lacking the pancreatic β-cell insulin receptor display a loss of first-phase glucose-stimulated insulin secretion but do not develop overt diabetes[9]. The activated receptors for insulin and Igf-1 phosphorylate various cellular substrates, including Irs-1 and Irs-2 (refs 10–12), which integrate the pleiotropic effects of insulin, Igf-1 and other cytokines on cellular function. Deletion of *Irs1* produces small, insulin-resistant mice with nearly normal glucose homeostasis due to compensatory β-cell expansion[13–16]. In contrast, mice lacking Irs-2 display nearly normal growth, but develop diabetes 8–10 weeks after birth accompanied by reduced β-cell mass and impaired function[13].

Here we have used a genetic approach to define the roles of Irs-1 and Irs-2 in somatic growth, peripheral carbohydrate metabolism and β-cell development and function. *Irs1*$^{+/-}$ and *Irs2*$^{+/-}$ mice were intercrossed to generate progeny with various states of Irs-1 and Irs-2 deficiency. To determine the contributions of the Igf-1 receptor during Irs-2–mediated β-cell expansion, we intercrossed *Irs2*$^{+/-}$ mice with *Igf1r*$^{+/-}$ mice. Our results suggest that Igf-1 receptors couple to Irs-2 to mediate islet development during embryogenesis and promote β-cell proliferation and survival during post-natal growth and in response to peripheral insulin resistance.

## Results

### Characteristics of mice lacking Irs-1 and Irs-2

We intercrossed *Irs1*$^{+/-}$*Irs2*$^{+/-}$ mice to produce 185 litters yielding 925 offspring representing 8 of 9 possible genotypes; Southern-blot analysis conducted at 2 weeks of age revealed no *Irs1*$^{-/-}$*Irs2*$^{-/-}$ mice. *Irs1*$^{+/-}$*Irs2*$^{-/-}$ and *Irs1*$^{-/-}$*Isr2*$^{+/-}$ mice were less frequent than expected (*Irs1*$^{+/-}$*Irs2*$^{-/-}$, 2.7% actual versus 12.5% expected; *Irs1*$^{-/-}$*Isr2*$^{+/-}$, 0.97% actual versus 12.5% expected). Consequently, mice of other genotypes were born with an altered frequency (wild type, 14.3% actual versus 6.25% expected; *Irs1*$^{+/-}$, 18.5% actual versus 12.5% expected; *Irs2*$^{+/-}$, 21.8% actual versus 12.5% expected; *Irs1*$^{-/-}$, 4% actual versus 6.25% expected; *Irs2*$^{-/-}$, 7.7% actual versus 6.25% expected; *Irs1*$^{+/-}$*Irs2*$^{+/-}$, 30.3% actual versus 25% expected). A similar distribution of genotypes was found for 108 embryos (embryonic day (E) 16.5–18.5) from 20 pregnant females and a small number of dead pups. These results suggest that *Irs1*$^{-/-}$*Irs2*$^{-/-}$ embryos are not viable, whereas *Irs1*$^{+/-}$*Irs2*$^{-/-}$ and *Irs1*$^{-/-}$*Irs2*$^{+/-}$ animals are viable but develop with a lower than expected frequency due to wastage before E16.5.

We generated growth curves based on daily weights from birth to 30 days of offspring from *Irs1*$^{+/-}$*Irs2*$^{+/-}$ intercrosses (Fig. 1*a*). Birth weights for *Irs1*$^{+/-}$, *Irs1*$^{-/-}$, *Irs2*$^{+/-}$ and *Irs2*$^{-/-}$ mice were consistent with previous reports[13,14]. Compound heterozygous mice (*Irs1*$^{+/-}$*Irs2*$^{+/-}$) were 75% the weight of wild-type animals. *Irs1*$^{+/-}$*Irs2*$^{-/-}$ mice were of similar size to *Irs1*$^{-/-}$ animals, whereas *Irs1*$^{-/-}$*Irs2*$^{+/-}$ mice were 70–75% smaller than normal littermates (Fig. 1*a*,*b*). *Irs1*$^{-/-}$*Irs2*$^{+/-}$ mice are among the smallest viable mice that have been generated from a variety of strategies aimed at deleting components of

[1]*Howard Hughes Medical Institute, Joslin Diabetes Center, Harvard Medical School, One Joslin Place, Boston, Massachusetts 02215, USA.* [2]*Current address: Department of Metabolic Medicine, Imperial College School of Medicine, Hammersmith Campus, Du Cane Road, London, W12ONN, UK. Correspondence should be addressed to M.F.W. (e-mail: morris.white@joslin.harvard.edu).*

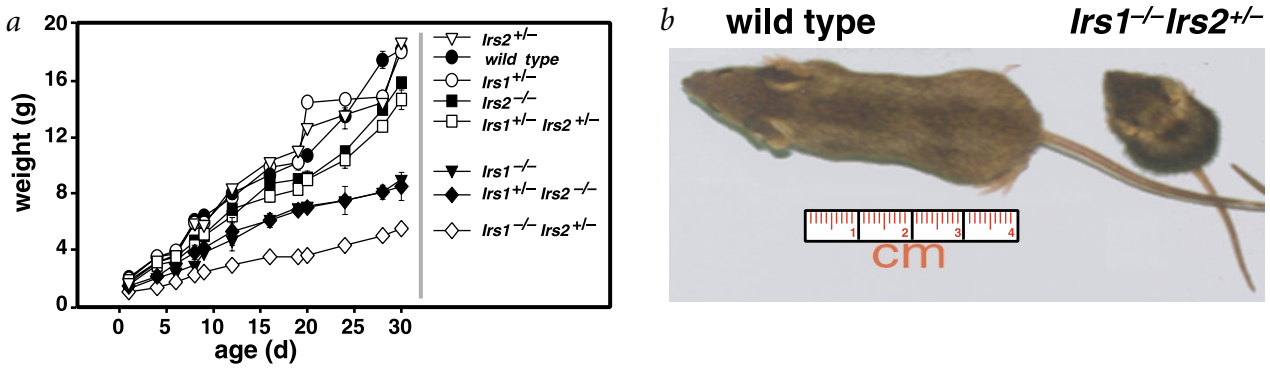


**Fig. 1** Growth characteristics of progeny of *Irs1*$^{+/-}$*Irs2*$^{+/-}$ intercross. ***a***, Growth curves showing mean weight±s.e.m. of animals of the various genotypes on a C57Bl/6×129SV background at the indicated ages (days). Data are from 170 litters with at least 4 animals per genotype. ***b***, A 30-day-old wild-type animal with an *Irs1*$^{-/-}$*Irs2*$^{+/-}$ littermate.

growth factor signalling pathways, and demonstrate that a single copy of *Irs2* promotes viability for at least one year.

## Metabolic consequences of Irs protein deletion

At 2–3 weeks of age, *Irs1*$^{+/-}$*Irs2*$^{-/-}$ mice had fasting blood sugars in excess of 300–400 mg/dl and thus were diabetic. By 4 weeks of age, the blood glucose values exceeded 500 mg/dl as mice displayed progressive polyuria (without ketonuria), polydyspsia and rarely survived beyond 5 weeks of age. This progression to the diabetic phenotype was quicker than that of *Irs2*$^{-/-}$ mice, in which overt diabetes did not usually present until after 10 weeks of age (Fig. 2*a*). In comparison, *Irs1*$^{+/-}$*Irs2*$^{+/-}$ and *Irs1*$^{-/-}$*Irs2*$^{+/-}$ mice had normal fasting blood glucose at four weeks of age (Fig. 2*a*). Glucose tolerance tests performed on four-week-old mice revealed that *Irs1*$^{+/-}$*Irs2*$^{-/-}$ mice were glucose intolerant, whereas *Irs2*$^{+/-}$, *Irs1*$^{+/-}$*Irs2*$^{+/-}$ and *Irs1*$^{-/-}$*Irs2*$^{+/-}$ mice displayed only mild glucose intolerance (Fig. 2*b*).

At four weeks, both *Irs1*$^{-/-}$ and *Irs2*$^{-/-}$ mice had elevated fasting insulin levels, consistent with compensated peripheral insulin resistance as previously reported[13], and *Irs1*$^{+/-}$*Irs2*$^{+/-}$ mice were also hyperinsulinaemic. Similarly, *Irs1*$^{-/-}$*Irs2*$^{+/-}$ mice displayed fasting hyperinsulinaemia, which maintained nearly

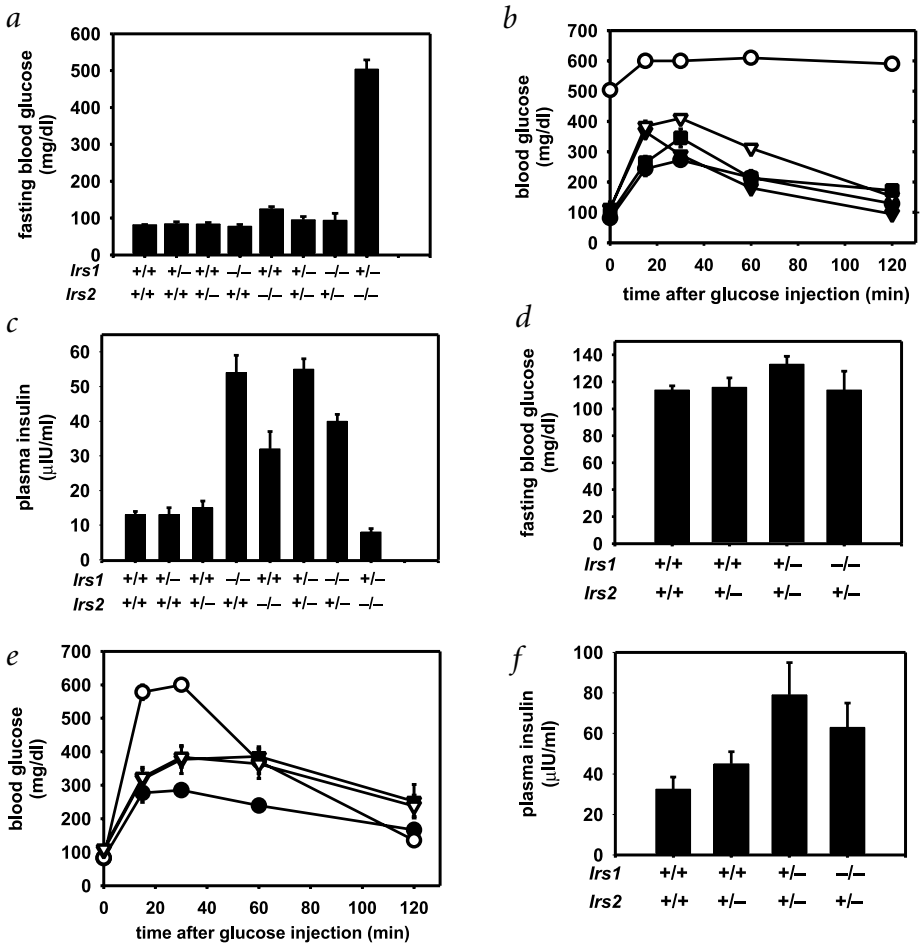


**Fig. 2** Metabolic characteristics of progeny of *Irs1*$^{+/-}$*Irs2*$^{+/-}$ intercross. ***a***, After a 15-h overnight fast, we determined blood glucose levels on 4-week-old animals. Results are mean values±s.e.m. for at least six animals of each genotype. ***b***, Glucose tolerance tests were performed after intraperitoneal loading with 2 g D-glucose per kg body weight on animals fasted overnight for 15 h (wild type, filled circles; *Irs2*$^{+/-}$, filled squares; *Irs1*$^{+/-}$*Irs2*$^{+/-}$, open triangles; *Irs1*$^{-/-}$*Irs2*$^{+/-}$, filled triangles; *Irs1*$^{+/-}$*Irs2*$^{-/-}$, open circles). ***c***, Serum insulin levels were measured by radioimmunoassay on 4-week-old anaesthetized animals after a 15-h overnight fast. ***d***, After a 15-h overnight fast, blood glucose levels were determined on 6-month-old animals. ***e***, Glucose tolerance tests were performed after intraperitoneal loading with 2 g D-glucose per kg body weight on fasted 6-month-old animals (wild type, filled circles; *Irs2*$^{+/-}$, open triangles; *Irs1*$^{+/-}$*Irs2*$^{+/-}$, filled triangles; *Irs1*$^{-/-}$*Irs2*$^{+/-}$, open circles). ***f***, After a 15-h overnight fast, serum insulin levels were measured by radioimmunoassay on 6-month-old anaesthetized animals. *b–f*, Results are the mean values±s.e.m. for at least four animals of each genotype.

© 1999 Nature America Inc. • http://genetics.nature.com

© 1999 Nature America Inc. • http://genetics.nature.com

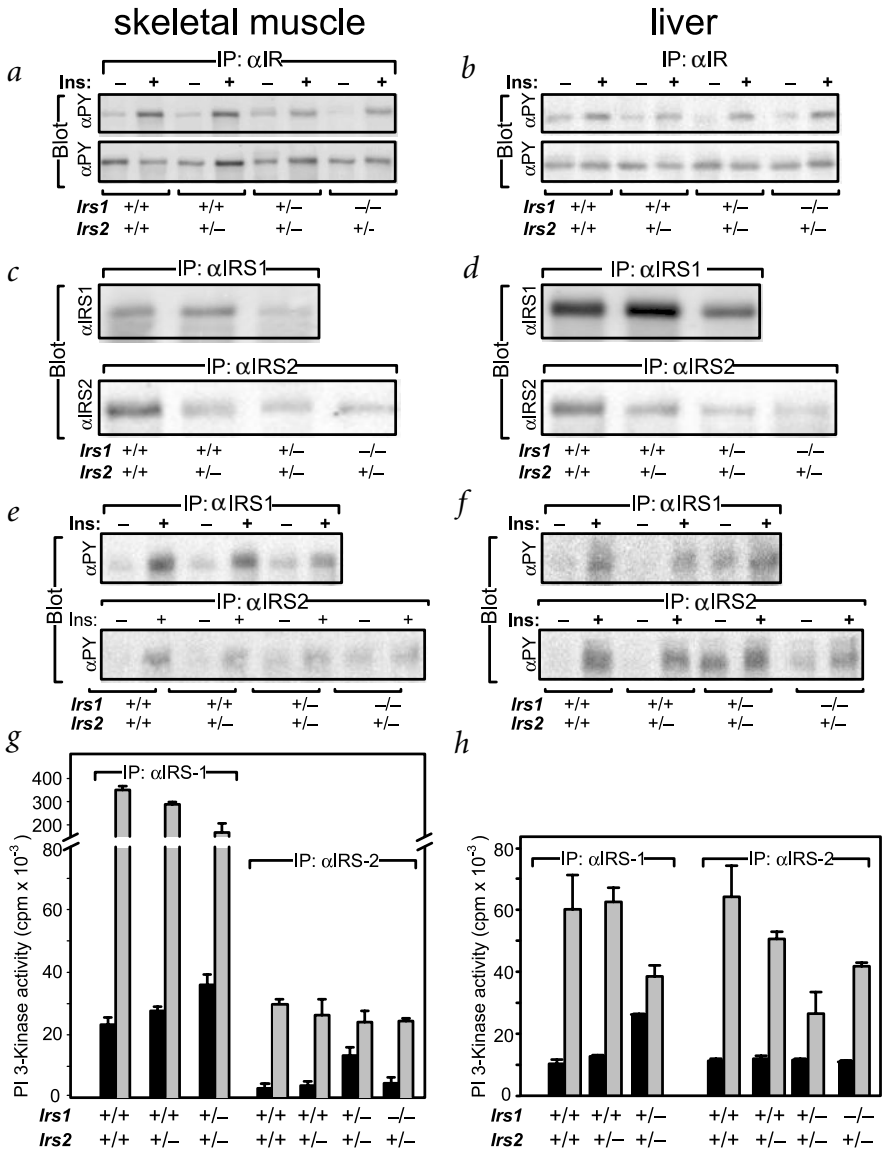


**Fig. 3** Insulin signalling in skeletal muscle and liver of progeny of an *Irs1*$^{+/-}$*Irs2*$^{+/-}$ intercross. Expression and tyrosine phosphorylation of the insulin receptor β-subunit in skeletal muscle (***a***) and liver (***b***) of animals of the indicated genotypes. Supernatants of muscle and liver homogenates containing total protein from untreated and insulin (Ins)-treated 4–8-week-old mice were immunoprecipitated with anti-IRβ antibody and blotted for either anti-phosphotyrosine (αPY) or IRβ (αIR). Expression of Irs-1 and Irs-2 in skeletal muscle (***c***) and liver (***d***) of animals is shown. Supernatants of muscle and liver homogenates of total protein (2 mg) were immunoprecipitated with either αIrs-1 or αIrs-2 antibody and blotted with the same antibody. *a–d*, Results are representative of three animals of each genotype. Tyrosine phosphorylation of Irs-1 and Irs-2 in skeletal muscle (***e***) and liver (***f***) is shown. Supernatants of muscle and liver homogenates containing total protein (2 mg) from untreated and insulin-treated 4–8-week-old mice were immunoprecipitated with αIrs-1 or αIrs-2 antibody blotted for antiphosphotyrosine (αPY). Immunoblots are representative of data from three animals per genotype. Insulin-stimulated PI-3K activation in muscle (***g***) and liver (***h***) is shown. Supernatants of muscle and liver homogenates containing total protein (2 mg) from untreated (black bars) and insulin-treated (grey bars) 4–8-week-old mice were immunoprecipitated (IP) in duplicate with the indicated antibody (αIrs-1 or αIrs-2); immunoprecipitates were assayed *in vitro* for PI-3 kinase activity. Data are the mean values±s.e.m. of two independent experiments and represent data from at least four animals of each genotype.

normal glucose tolerance against peripheral insulin resistance (Fig. 2*c*). By contrast, *Irs1*$^{+/-}$*Irs2*$^{-/-}$ mice had lower fasting insulin levels than wild-type animals (Fig. 2*c*). Insulin levels in randomly fed *Irs1*$^{+/-}$*Irs2*$^{-/-}$ mice were lower than those seen in wild-type mice, demonstrating the presence of relative insulin insufficiency (data not shown). By these criteria, *Irs2*$^{+/-}$ mice had no insulin resistance at this age as reported[13].

*Irs1*$^{-/-}$*Irs2*$^{+/-}$ mice maintained normal fasting blood sugars when followed up to six months of age (Fig. 2*d*). These mice displayed impaired glucose tolerance at early time points during a glucose tolerance test, with glucose concentrations returning to normal by 120 minutes (Fig. 2*e*). Similar analysis of *Irs2*$^{+/-}$ and *Irs1*$^{+/-}$*Irs2*$^{+/-}$ mice at six months showed that glucose tolerance had deteriorated, whereas fasting blood sugars remained normal (Fig. 2*e*). At six months of age, *Irs2*$^{+/-}$ mice displayed fasting hyperinsulinaemia and *Irs1*$^{+/-}$*Irs2*$^{+/-}$ mice had slightly higher insulin levels consistent with an age-related development of insulin resistance (Fig. 2*f*). *Irs1*$^{-/-}$*Irs2*$^{+/-}$ mice were also hyperinsulinaemic at six months of age, demonstrating that a single copy of *Irs2* was sufficient to maintain appropriate β-cell compensation in the presence of insulin resistance (Fig. 2*f*).

## Insulin signalling pathways in Irs-deficient mice

We examined insulin-stimulated tyrosine phosphorylation and PI-3 kinase activity in skeletal muscle and liver. Signalling events in *Irs1*$^{+/-}$*Irs2*$^{-/-}$ mice were omitted because hyperglycaemia and their short lifespan made meaningful analysis of genetic manipulation of these parameters impossible. Insulin receptor levels and activation as assessed by expression and tyrosine autophosphorylation of the β-subunit were comparable in liver and skeletal muscle in all genotypes studied at four months of age (Fig. 3*a*,*b*). Expression of Irs-1 or Irs-2 was reduced (50%) or undetectable, consistent with the genotype of the individual mice; there was no evidence for compensatory overexpression (Fig. 3*c*,*d*, and data not shown).

Irs-2 tyrosine phosphorylation was reduced in liver and muscle of *Irs1*$^{+/+}$*Irs2*$^{+/-}$ mice, consistent with reduced expression, whereas Irs-1 tyrosine phosphorylation was comparable to that of controls (Fig. 3*e*,*f*). By contrast, basal tyrosine phosphorylation of both Irs-1 and Irs-2 was elevated in liver of *Irs1*$^{+/-}$*Irs2*$^{+/-}$ mice (Fig. 3*e*,*f*). Elevated Irs-2 tyrosine phosphorylation was also detected in liver of *Irs1*$^{-/-}$*Irs2*$^{+/-}$ mice (Fig. 3*f*).

We assessed insulin-stimulated PI-3 kinase activity in Irs-1 and Irs-2 immunoprecipitates from both liver and muscle at

© 1999 Nature America Inc. • http://genetics.nature.com

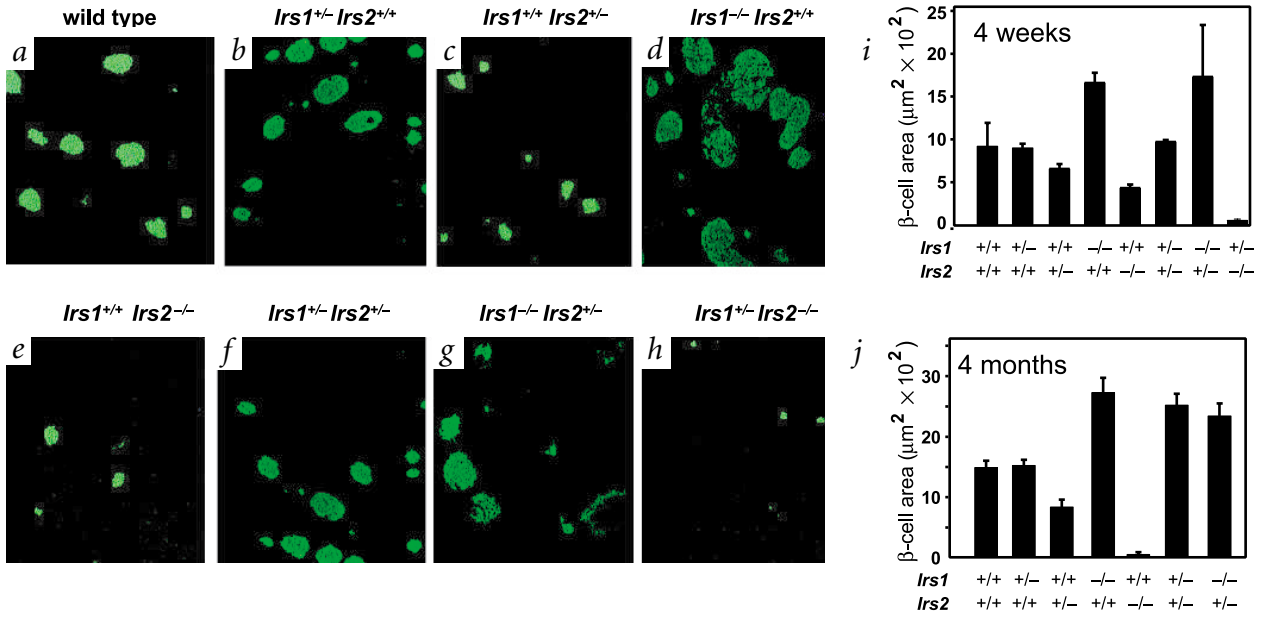


**Fig. 4** Islet morphology and β-cell analysis in progeny of *Irs1*$^{+/-}$*Irs2*$^{+/-}$ intercross. ***a–h***, Immunostaining of insulin in β-cells of pancreas sections from four-week-old mice. Permeabilized, paraffin-embedded pancreas sections (5 μm) were incubated with monoclonal anti-insulin antibodies. Staining was revealed by fluoroscein anti-mouse antibodies. Images of representative fields were captured at a magnification of ×10. ***i,j***, Quantitation of β-cell area in four-week and four-month-old mice. Pancreas sections immunostained for insulin were viewed using a Zeiss Axiovert Microscope and video camera. Results are mean values±s.e.m. of at least four animals of each genotype.

four months of age. In *Irs2*$^{+/-}$ mice there was a reduction in Irs-2–associated PI-3 kinase activity on insulin stimulation in the liver, whereas the activity in muscle was nearly normal compared with wild-type controls (Fig. 3*g*,*h*). By contrast, Irs-1–associated PI-3 kinase activity decreased slightly in muscle of *Irs2*$^{+/-}$ mice, despite the normal expression of Irs-1 and normal insulin receptor function (Fig. 3*g*,*h*). In *Irs1*$^{-/-}$*Irs2*$^{+/-}$ mice, insulin-stimulated Irs-2–associated PI-3 kinase activity was largely preserved, especially in skeletal muscle (Fig. 3*g*). In *Irs1*$^{+/-}$*Irs2*$^{+/-}$ mice, however, there was less of an increase in Irs-1–associated PI-3 kinase activity in insulin-stimulated muscle and liver (Fig. 3*g*,*h*) and in Irs-2–associated PI-3 kinase activity in muscle (Fig. 3*g*). This reduced increase in insulin-stimulated PI-3 kinase activity in *Irs1*$^{+/-}$*Irs2*$^{+/-}$ mice is due in part to elevated basal activity of the enzyme in Irs-1 and Irs-2 immunoprecipitates from muscle and liver. These results suggest there is a complex interplay between Irs-1 and Irs-2 in the appropriate regulation of PI-3 kinase activation in both liver and muscle.

## Islet morphology in mice lacking Irs proteins

We have previously implicated Irs-2–dependent signalling pathways in the β-cell compensatory response to insulin resistance, possibly by regulating differentiation, proliferation or survival of β-cells. Therefore, the rapid onset of diabetes in *Irs1*$^{+/-}$*Irs2*$^{-/-}$ mice, but not in *Irs1*$^{-/-}$*Irs2*$^{+/-}$ mice, prompted us to analyse islet morphology. β-cell area in multiple pancreas

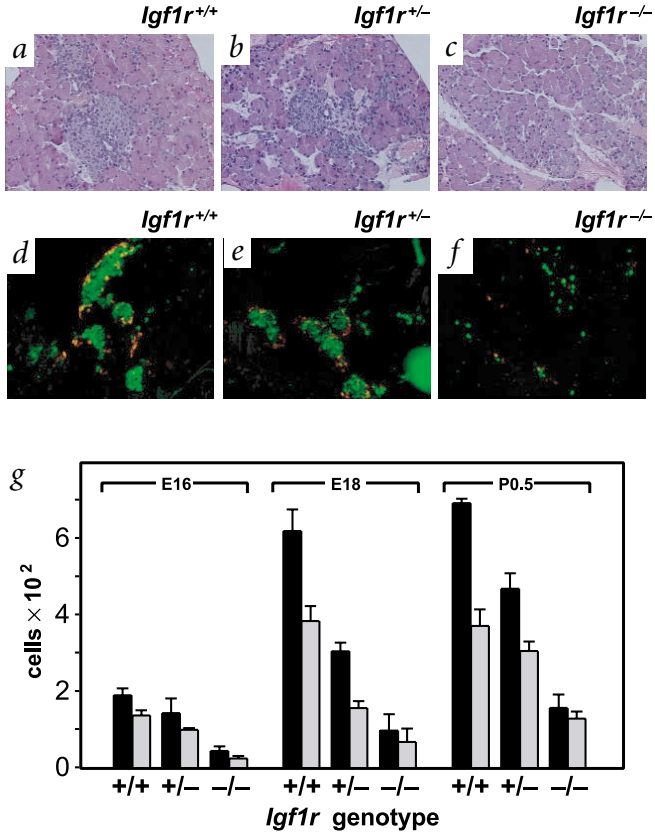


**Fig. 5** Islet morphology and β-cell mass in *Igf1r*$^{-/-}$ mice. ***a–c***, Pancreas sections (5 μm) from newborn pups (post-natal day 0.5) were stained with haematoxylin and eosin and photographed at a magnification of ×20. ***d–f***, Pancreas sections obtained from E18 embryos were co-immunostained for insulin and glucagon. Insulin-positive cells were revealed by fluorescein-labelled secondary antibodies (green); glucagon-containing cells were detected by rhodamine-labelled secondary antibodies (red). Images were collected separately at a magnification of ×20 and superimposed. ***g***, α- and β-cell areas in embryos and newborns were quantitated from pancreas co-immunostained for insulin, glucagon and amylase. Results are the mean values±s.e.m. for at least three animals of each genotype. Grey bars, α-cell numbers; black bars, β-cell numbers.

© 1999 Nature America Inc. • http://genetics.nature.com

© 1999 Nature America Inc. • http://genetics.nature.com

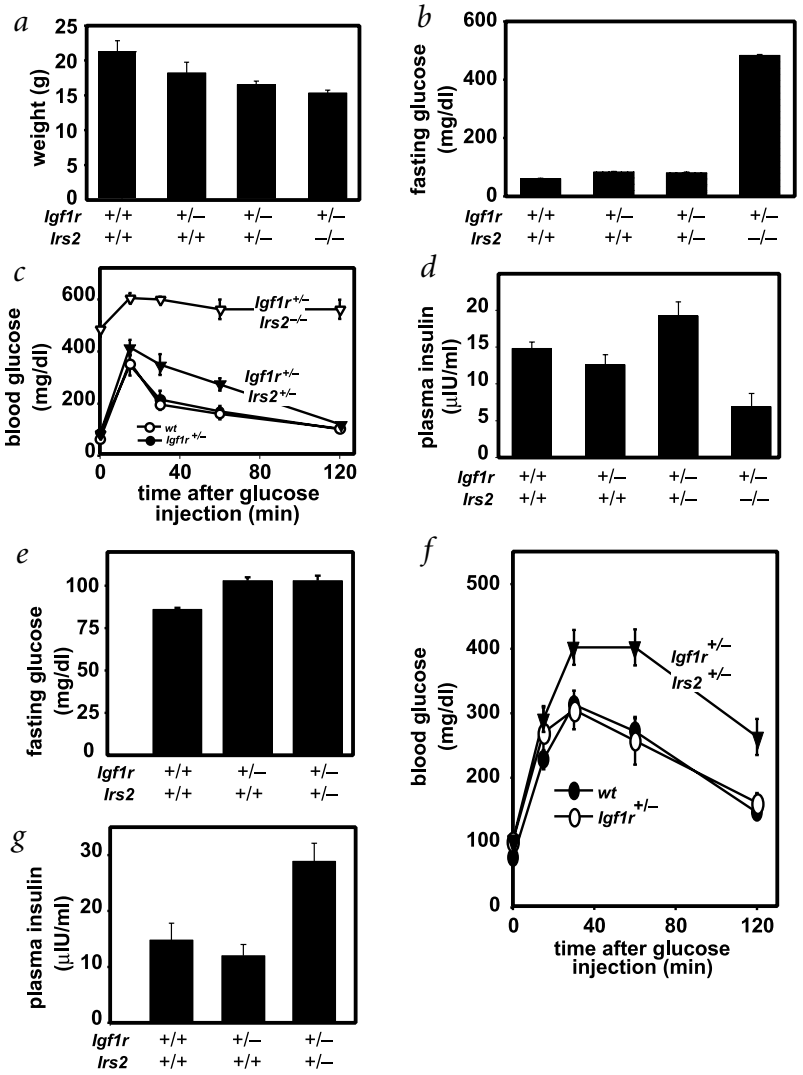


**Fig. 6** Weight and metabolic characteristics of progeny of *Igf1r*$^{+/-}$*Irs2*$^{+/-}$ intercross. ***a***, Mean weights±s.e.m. of 30-day-old mice. Data are from ten litters with at least four animals per genotype. ***b***, After a 15-h overnight fast, blood glucose levels were determined on 4-week-old animals. Results are mean values±s.e.m. for at least six animals of each genotype. ***c***, Glucose tolerance tests were performed after intraperitoneal loading with 2 g D-glucose per kg body weight on fasted 4-week-old animals of the indicated genotypes. ***d***, Serum insulin levels were measured by radioimmunoassay on 4-week-old anaesthetized animals after a 15-h overnight fast. ***e***, After a 15-h overnight fast, blood glucose levels were determined on 4-month-old animals of the indicated genotype. ***f***, Glucose tolerance tests were performed after intraperitoneal loading with 2 g D-glucose per kg body weight on fasted 4-month-old animals of the indicated genotypes. ***g***, Serum insulin levels were measured by radioimmunoassay on 4-month-old anaesthetized animals after a 15-h overnight fast. *c–g*, Results are mean values±s.e.m. for at least four animals of each genotype.

cross-sections from 4-week-old *Irs1*$^{+/-}$*Irs2*$^{-/-}$ mice was reduced more than 90% (Fig. 4*a*,*h*,*i*). Analysis of *Irs1*$^{+/-}$*Irs2*$^{-/-}$ mice at E18.5 (when islet morphology is initially established) revealed a reduced β-cell number, confirming that deletion of Irs-2 impaired β-cell neogenesis and proliferation during development (wild type, $6.1\times10^2$ cells versus *Irs1*$^{+/-}$*Irs2*$^{-/-}$, $1.2\times10^2$ cells, n=2). These findings are consistent with the relative hypoinsulinaemia seen in these animals and explain provisionally their rapid development of diabetes.

*Irs1*$^{-/-}$*Irs2*$^{+/-}$ mice displayed insulin resistance and somatic growth retardation, but relatively normal islet morphology (Fig. 4*g*). Compared with wild-type mice, the average β-cell area in *Irs1*$^{-/-}$*Irs2*$^{+/-}$ mice was increased 1.8-fold at 4 weeks and 4 months of age (Fig. 4*a*,*g*,*i*,*j*). These findings suggest that Irs-2–dependent signalling pathways, but not Irs-1 pathways, sustain normal islet development and appropriate compensatory responses during peripheral insulin resistance.

Examination of islets from *Irs1*$^{+/+}$*Irs2*$^{+/-}$ mice, which display little peripheral insulin resistance, revealed a 25% and 36% reduction in β-cell area at 4 weeks and 4 months of age, respectively (Fig. 4*c*,*i*,*h*). By contrast, β-cell area in *Irs1*$^{+/-}$*Irs2*$^{+/-}$ mice, which display peripheral insulin resistance, was normal at 4 weeks of age and elevated 1.7-fold at 4 months of age, reaching levels similar to those observed in *Irs1*$^{-/-}$*Irs2*$^{+/+}$ mice (Fig. ,4*f*,*i*,*j*). Thus, expression of Irs-2 may be essential for β-cell expansion during the compensatory response to peripheral insulin resistance.

## β-cell development in *Igf1r*$^{-/-}$ mice

To further characterize the signals that activate Irs-2 pathways in β-cell function, we analysed islet morphology and glucose homeostasis in *Igf1r*$^{-/-}$ mice or mice heterozygous for *Igf1r* and lacking *Irs2*. As previously reported, deletion of the Igf-1 receptor causes neonatal death within minutes of birth, probably due to respiratory failure, which precludes detailed metabolic analysis[7]. Close monitoring of several litters at birth revealed elevated blood glucose levels in *Igf1r*$^{-/-}$ pups (*Igf1r*$^{-/-}$, 262±12 mg/ml versus wild type, 62.8±2.8 mg/dl, n=4).

In the developing mouse pancreas, endocrine-positive cells occur at E9.5, form interstitial clusters adjacent to the ductal epithelia at day 14.5 and proliferate and reorganize to form mature islets during the remaining 4 days of gestation[17]. Haematoxylin and eosin staining of pancreatic sections of *Igf1r*$^{-/-}$ mice revealed that morphological development of the exocrine tissue and organization into acini was normal at birth (Fig. 5*a–c*). In addition, exocrine pancreas of *Igf1r*$^{-/-}$ mice stained positively for amylase (data not shown), confirming functional development of this tissue. Compared with wild-type embryos, immunohistochemical analysis of pancreas sections from *Igf1r*$^{+/-}$ or *Igf1r*$^{-/-}$ mice revealed a 50% or 85% reduction of both insulin- and glucagon-positive cells, respectively, at E16, E18.5 and P0.5 (Fig. 5*d–g*). Moreover, α-cells and β-cells of *Igf1r*$^{-/-}$ pancreas failed to organize into spherical structures characteristic of maturing islets (Fig. 5*d–g*). Even at birth, islets in these animals were detected as strings of disorganized cells, lacking typical islet morphology. Thus, like Irs-2, Igf1r has a critical role in the development of normal, functional islets.

## Phenotypes in progeny of the *Igf1r*$^{+/-}$*Irs2*$^{+/-}$ intercross

To further characterize the effect of the Igf-1 receptor on glucose homeostasis, we intercrossed *Igf1r*$^{+/-}$*Irs2*$^{+/-}$ mice. At 30

© 1999 Nature America Inc. • http://genetics.nature.com

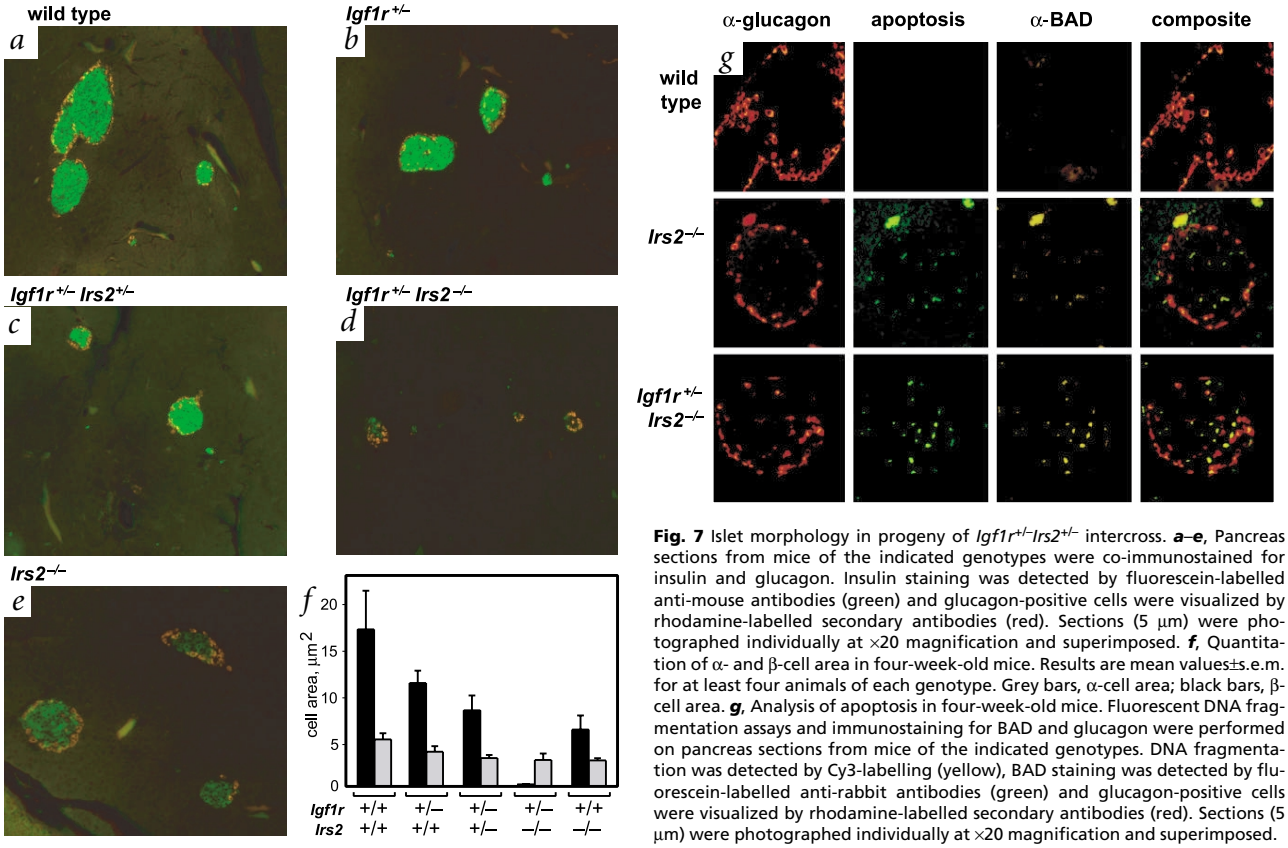


**Fig. 7** Islet morphology in progeny of *Igf1r*$^{+/-}$*Irs2*$^{+/-}$ intercross. ***a*–*e***, Pancreas sections from mice of the indicated genotypes were co-immunostained for insulin and glucagon. Insulin staining was detected by fluorescein-labelled anti-mouse antibodies (green) and glucagon-positive cells were visualized by rhodamine-labelled secondary antibodies (red). Sections (5 µm) were photographed individually at ×20 magnification and superimposed. ***f***, Quantitation of α- and β-cell area in four-week-old mice. Results are mean values±s.e.m. for at least four animals of each genotype. Grey bars, α-cell area; black bars, β-cell area. ***g***, Analysis of apoptosis in four-week-old mice. Fluorescent DNA fragmentation assays and immunostaining for BAD and glucagon were performed on pancreas sections from mice of the indicated genotypes. DNA fragmentation was detected by Cy3-labelling (yellow), BAD staining was detected by fluorescein-labelled anti-rabbit antibodies (green) and glucagon-positive cells were visualized by rhodamine-labelled secondary antibodies (red). Sections (5 µm) were photographed individually at ×20 magnification and superimposed.

days of age, *Igf1r*$^{+/-}$, *Igf1r*$^{+/-}$*Irs2*$^{+/-}$ and *Igf1r*$^{+/-}$*Irs2*$^{-/-}$ mice had nearly normal weights compared with wild-type animals (Fig. 6*a*). At 2 weeks, *Igf1r*$^{+/-}$*Irs2*$^{-/-}$ mice had fasting blood glucose in excess of 300–400 mg/dl; at 4 weeks, blood glucose levels exceeded 500 mg/dl (Fig. 6*b*). Similar to *Irs1*$^{+/-}$*Irs2*$^{-/-}$ animals, these mice developed polyuria, polydypsia, weight loss and rarely survived beyond five weeks of age. At this age, fasting blood glucose was normal in *Igf1r*$^{+/-}$ and *Igf1r*$^{+/-}$*Irs2*$^{+/-}$ mice (Fig. 6*b*).

*Igf1r*$^{+/-}$*Irs2*$^{-/-}$ mice were glucose intolerant, whereas *Igf1r*$^{+/-}$*Irs2*$^{+/-}$ mice had mild impairment of glucose disposal; *Igf1r*$^{+/-}$ mice did not differ from wild-type animals (Fig. 6*c*). *Igf1r*$^{+/-}$*Irs2*$^{-/-}$ mice were hypoinsulinaemic after fasting compared with wild-type animals, whereas *Igf1r*$^{+/-}$*Irs2*$^{+/-}$ mice had mild hyperinsulinaemia and *Igf1r*$^{+/-}$ mice were slightly hypoinsulinaemic (Fig. 6*d*). Examination of these parameters at four months of age revealed that *Igf1r*$^{+/-}$ mice had normal fasting blood glucose levels, whereas glucose tolerance and fasting hyperinsulinaemia developed in *Igf1r*$^{+/-}$*Irs2*$^{+/-}$ mice (Fig. 6*e–g*).

*Igf1r*$^{+/-}$*Irs2*$^{-/-}$ mice displayed a reduction in β-cell area, with insulin-positive cells representing less than 2% of those seen in wild-type animals (Fig. 7*a*,*d*). This reduction in β-cells was more pronounced than the 50–60% reduction observed in *Irs2*$^{-/-}$ mouse islets (Fig. 7*e*,*f*). Glucagon-positive cells in *Igf1r*$^{+/-}$*Irs2*$^{-/-}$ mice were reduced by only 50%, demonstrating that defective Igf1r→Irs-2 signalling has more severe consequences for β-cell development and maintenance (Fig. 7*f*). Additionally, analysis of *Igf1r*$^{+/-}$ and *Igf1r*$^{+/-}$*Irs2*$^{+/-}$ mice revealed a compromised β-cell mass, with a 30–50% reduction in insulin-positive cell area in these animals (Fig. 7*b*,*c*,*f*). Thus, these observations suggest that Igf1r→Irs-2 signalling pathways are critical for β-cell proliferation and function.

## Role of Igf1r→Irs-2 signalling pathway in β-cell survival

Insulin-like growth factors prevent induced apoptosis in a variety of cell types[18]. In addition, IRS-dependent pathways have been shown to mediate the anti-apoptotic effects of IGF-1 (ref. 19). As the determinants of β-cell mass are thought to involve a combination of new islet formation and proliferation of pre-existing islets balanced by developmentally regulated β-cell apoptosis[20,21], we examined islets from the offspring of *Igf1r*$^{+/-}$*Irs2*$^{+/-}$ mice for the presence of apoptosis and expression of the pro-apoptotic protein BAD (ref. 22). Increased numbers of apoptotic cells were present in the islets of *Irs2*$^{-/-}$ and *Igf1r*$^{+/-}$*Irs2*$^{-/-}$ mice compared with wild-type animals (Fig. 7*g*). There was also increased expression of BAD in the islets of these animals (Fig. 7*g*). Apoptotic nuclei and BAD-positive cells co-localized inside the outer ring glucagon-positive cells (Fig. 7*g*). These findings suggest that increased apoptosis might underlie the β-cell failure in these mice.

## Discussion

Irs-1 and Irs-2 mediate the effects of insulin and Igf-1 on embryonic development, post-natal somatic growth and glucose homeostasis. No embryos (16.5 days or older) null for both genes have been detected in our studies, suggesting that Irs-1 and Irs-2 are critical for embryonic development. Irs-1 has a predominant role in somatic growth, as deletion of *Irs1* reduces embryonic and neonatal growth by 40%, whereas deletion of *Irs2* reduces growth by 10%. *Irs1*$^{+/-}$*Irs2*$^{-/-}$ mice are approximately 60% the size of wild-type animals, whereas *Irs1*$^{-/-}$*Irs2*$^{+/-}$ mice are only 30% the size of controls, implicating Irs-1 as the principal element by which Igf-1 mediates somatic growth. Moreover, our studies indicate that Irs-2 may participate in somatic growth, but cannot fully replace Irs-1. These findings

© 1999 Nature America Inc. • http://genetics.nature.com

© 1999 Nature America Inc. • http://genetics.nature.com

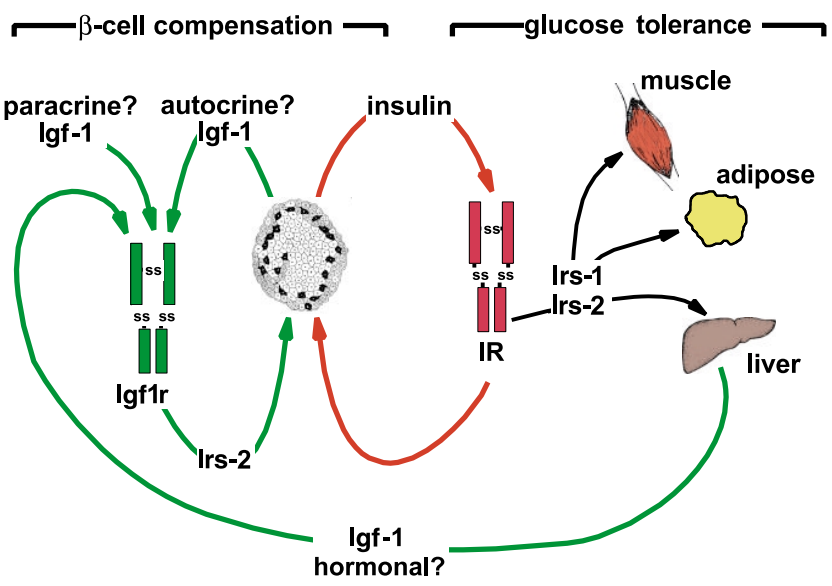


**Fig. 8** A model depicting the central role of Irs-2 signalling pathways in the maintenance of normal glucose homeostasis. Igf1r couples to Irs-2 in the pancreatic islet to mediate β-cell development, proliferation and survival. Irs-2–mediated pathways are also required for β-cell compensation in response to peripheral insulin resistance. In insulin target tissues, both Irs-1 and Irs-2 participate in mediating insulin action on cellular function. Our results suggest that alterations in the balance of these proteins in peripheral tissues may lead to insulin resistance.

are consistent with *in vitro* observations that Irs-2 fails to fully reconstitute the mitogenic effects of Igf-1 in $Irs1^{-/-}$ fibroblasts or 32D cells[23].

Although Irs-1 has a predominant role in somatic growth and deletion of either Irs-1 or Irs-2 causes peripheral insulin resistance, our data suggest that Irs-2–dependent mechanisms may be more critical in glucose homeostasis. Indeed, insulin may regulate carbohydrate metabolism in the liver via Irs-2 rather than Irs-1 (ref. 24). Additionally, Irs-2, downstream of the Igf-1 receptor, is critical for the development and maintenance of appropriate β-cell mass. Thus, Irs-2 signalling pathways have evolved as a common element controlling insulin production and glucose homeostasis. This hypothesis is highlighted by the finding that $Irs1^{-/-}Irs2^{+/-}$ mice develop mild glucose intolerance due to compensated peripheral insulin resistance, whereas $Irs1^{+/-}Irs2^{-/-}$ and $Igf1r^{+/-}Irs2^{-/-}$ mice die from diabetes by six weeks of age due to β-cell insufficiency.

The distinct physiological functions of Irs-1 and Irs-2 might be explained partially by tissue-specific differences in expression of these proteins; however, both Irs-1 and Irs-2 are expressed in most tissues, including liver, muscle and both rodent islets and mouse β-cells[12,25–27]. Thus, it is unlikely that the absolute expression of either of these proteins in a given tissue provides a complete explanation for their physiological differences. By contrast, the presence of the KRLB domain in Irs-2, which binds the regulatory loop of the insulin receptor, might direct biological specificity[28,29]. It is possible that direct cross-talk between Irs-1 and Irs-2 may be required to appropriately regulate pathways of insulin and Igf-1 action. Our observations suggest a complex interplay between Irs-1 and Irs-2 in the regulation of downstream signalling in liver and muscle; alterations in the balance of these signalling molecules may contribute significantly to pathogenesis of peripheral insulin resistance.

The extracellular ligands and intracellular signalling pathways involved in islet development, growth and survival are poorly characterized, but these signals are ultimately transmitted to a hierarchy of transcription factors which regulate differentiation and maintenance of β-cells[30–34]. Our results suggest that the Igf1r→Irs-2 signalling pathway may partially regulate these processes. Endocrine cells develop poorly in $Igf1r^{-/-}$ embryos and fail to form typical islets. By contrast, islets form in $Irs2^{-/-}$ mice, but β-cell mass is reduced at birth and remains inadequate to compensate for peripheral insulin resistance. Moreover, the effect of *Irs2* disruption is more profound in $Igf1r^{+/-}$ mice, suggesting an important role for the Igf1r→Irs-2 signalling pathway. Although $Igf1r^{-/-}$ embryos are reduced in size, the overall developmental delay in ossification and neuronal development is only about 1–2 days, suggesting that the defects in β-cell development are a specific effect of the genetic lesion rather than a global developmental retardation[7,35]. In addition, increased numbers of apoptotic cells and increased expression of the pro-apoptotic protein BAD in the islets of $Irs2^{-/-}$ and $Igf1r^{+/-}Irs2^{-/-}$ mice suggest that Igf1r→Irs-2 pathways might protect β-cells from apoptosis. Thus, decreased survival represents one mechanism underlying the β-cell defect in these animals.

The relation between β-cell function and peripheral tissues in the development of diabetes is well established[36]. Our genetic models reinforce this concept and emphasize β-cell dysfunction as a critical determinant in the development of diabetes. We have developed mouse models of diabetes in which the disease ensues as a consequence of a fundamental defect in β-cell development: $Irs2^{-/-}$, $Irs1^{+/-}Irs2^{-/-}$ and $Igf1r^{+/-}Irs2^{-/-}$ mice are born with insufficient β-cells to maintain proper glucose homeostasis. Moreover, based on our analysis of these mice at 4–6 weeks, they do not possess the mechanisms to generate new β-cells or to sustain survival of existing β-cells. Therefore, when the β-cell defect combines with peripheral insulin resistance, insulin-producing cells 'burn out' within a few weeks and overt diabetes ensues. Thus, these mouse models emphasize the fundamental necessity of Igf1r→Irs-2 signalling in the development and maintenance β-cell function (Fig. 8).

We have also generated models that emphasize the interplay between peripheral insulin resistance and the β-cell response. $Irs1^{+/-}Irs2^{+/-}$ and $Irs1^{-/-}Irs2^{+/-}$ mice are born with a relatively normal β-cell mass. Due to the reduced expression of Irs-1 and Irs-2 in peripheral tissues, these lean animals are insulin-resistant and become mildly glucose intolerant with age; however, β-cell compensation is robust and diabetes does not develop. Therefore, these findings demonstrate that partial defects in both the β-cell and peripheral tissues underlie age-dependent development of diabetes. Thus, $Irs1^{+/-}Irs2^{+/-}$ and $Irs1^{-/-}Irs2^{+/-}$ mice represent polygenic models that may resemble non-

© 1999 Nature America Inc. • http://genetics.nature.com

insulin dependent diabetes mellitus (NIDDM), in which the combination of two mild defects in insulin signalling produces insulin resistance and progression to diabetes.

Our results demonstrate that the Irs protein signalling system, and in particular Irs-2, has a role in integrating carbohydrate metabolism in peripheral tissues with β-cell function. The characteristics of the mouse models developed from our studies may enable identification of the molecular defects that determine diabetes in humans, particularly at the level of the β-cell itself. These models suggest that lesions in the Irs-2 signalling pathway are a major factor in both β-cell dysfunction and peripheral insulin resistance. To date, genetic analysis of diabetic populations has found no significant polymorphisms in *Irs2* (ref. 12); however, our observations suggest that other mechanisms such as a reduced expression of Irs-2 or the IGF-1 receptor, particularly in the β-cell, may predispose individuals to diabetes. Our models provide unique tools to identify and characterize β-cell growth and survival pathways and present opportunities to link signalling pathways to the regulation of transcription factors that promote β-cell development and function.

## Methods

**Generation of *Irs1*$^{+/-}$*Irs2*$^{+/-}$ mice.** We generated *Irs1*$^{+/-}$ and *Irs2*$^{+/-}$ mice using described gene targeting strategies[13]. Both mouse lines were maintained on a mixed C57Bl/6×129Sv genetic background to facilitate a comparative analysis. To obtain mice that are compound heterozygotes for null alleles of *Irs1* and *Irs2*, we intercrossed *Irs1*$^{+/-}$ with *Irs2*$^{+/-}$ animals. *Irs1*$^{+/-}$*Irs2*$^{+/-}$ mice were viable and obtained with the expected mendelian frequency (12.5%). *Irs1*$^{+/-}$*Irs2*$^{+/-}$ mice were fertile and intercrossed to obtain progeny of all combinations of deletion of *Irs1* and *Irs2*. We genotyped animals at 1–2 weeks by Southern blot on genomic DNA obtained from tail samples as described[13].

**Generation of *Igf1r*$^{-/-}$ and *Igf1r*$^{+/-}$*Irs2*$^{+/-}$ mice.** The generation and genotyping of *Igf1r*$^{-/-}$ mice has been described[7]. To obtain *Igf1r*$^{+/-}$*Irs2*$^{+/-}$ mice, we intercrossed *Irs2*$^{+/-}$ and *Igf1r*$^{+/-}$ mice. *Igf1r*$^{+/-}$*Irs2*$^{+/-}$ mice were viable and obtained with expected mendelian frequency (12.5%). *Igf1r*$^{+/-}$*Irs2*$^{+/-}$ mice were fertile and intercrossed to obtain progeny of all combinations of deletion of *Igf1r* and *Irs2*. Genotyping of E16–18.5 embryos and 2-week-old animals was performed by Southern blot as described[7].

**Metabolic studies.** Animals were maintained on a normal light/dark cycle and handled in accordance with Joslin Diabetes Center Animal Care and Use Committee protocols. We determined glucose levels of blood from mouse tails using a Glucometer Elite glucometer (Bayer). We obtained blood for plasma insulin levels by retroorbital bleeds on anaesthetized mice or by tail bleeds. Immunoreactive insulin levels were measured either by radioimmunassay using rat insulin (Linco) as a standard or using an ELISA (CrystalChem) with mouse insulin as a standard. We performed glucose tolerance tests on animals after a 15-h overnight fast as described[13].

**Immunoprecipitation, western-blot analysis and PI-3K assays.** Liver and muscle tissue lysates were removed and homogenized at 4 °C as described[13]. The homogenates were allowed to solubilize for 1 h at 4 °C and clarified by centrifugation at 15,000 r.p.m. for 30 min. Supernatants containing total protein (2 mg) were immunoprecipitated with either an anti-Irs-2 antibody (residues 619–746 of mouse Irs-2), anti-Irs-1 antibody (residues 735–900 of mouse Irs-1) or anti-IR-β antibody. Blots were probed with polyclonal anti-Irs-1, anti-Irs-2, monoclonal anti-phosphotyrosine (clone 4G10) antibodies and detected by either $^{125}$I-protein A (ICN Biochemicals) or enhanced chemiluminescence. For PI-3 kinase enzymatic assays, we injected human insulin (5 units) as a bolus into the inferior vena cava of anaesthetized mice, and removed liver, gastrocnemius and quadriceps muscles at 1, 2.5 and 3 min after insulin injection. They were homogenized, solubilized and supernatants containing total protein (2 mg) immunoprecipitated for 2 h with anti-Irs-2 or anti-Irs-1 antibody as above. Immune complexes were collected, washed and the PI-3 kinase reaction performed as described[13]. We quantified $^{32}$P incorporation using a Phosphorimager (Molecular Dynamics).

**Immunohistochemistry of pancreas, quantitation of β-cells and detection of apoptosis.** For analysis of adult pancreases, animals were killed by overdose of sodium amytal. Each pancreas was removed, cleared of fat and spleen, weighed and fixed overnight in Bouin's solution. We embedded tissues in paraffin and mounted consecutive sections (5 μm) on slides. Following re-hydration and permeabilization (0.1% Triton X-100), sections were immunostained for α-cells using mouse monoclonal anti-glucagon antibodies (Sigma). β-cells were immunostained using either guinea pig anti-insulin (Linco) or mouse anti-insulin antibodies (Sigma). Detection was performed using rhodamine and fluorescein antibodies (Jackson Immunoresearch). We incubated sections briefly in DAPI (0.01%) to reveal total cell nuclei. BAD staining was performed with a rabbit polyclonal antibody (Santa Cruz) with detection as above. We identified apoptotic cells in de-paraffinized pancreatic sections using a fluorescent DNA fragmentation detection assay (Oncogene Research) and performed co-localization with glucagon and BAD staining as above.

For analysis of embryonic pancreas, we killed pregnant mice by administration of an overdose of sodium amytal on day E16.5 or E18.5. Fetuses were placed in phosphate-buffered saline (PBS) and the dorsal and ventral pancreatic buds carefully dissected and fixed in Bouin's for 3–4 h. Tissue specimens were washed in PBS and transferred to 10% buffered formalin. Pancreas from each neonate was also collected and fixed by the same procedure. We immunostained paraffin-embedded sections as described above. To assess the morphology and mass of the exocrine pancreas in these embryos, we also stained these sections with a rabbit anti-amylase antibody (Sigma).

For quantitation of β-cell area, sections were viewed using a Zeiss Axiovert S100 TV microscope and video camera at a magnification of ×20. Two sections of each pancreas were covered systematically by accumulating images from 8 non-overlapping fields of $1.5\times10^6$ μm$^2$. Analyses of β-cell area and size were performed using Openlab image analysis software (Improvision Imaging). This software calibrated the magnification of each micrograph. The percentage of cells positive for insulin or glucagon was calculated and corrected for pancreatic weight. For analysis of β-cells in embryonic or neonatal pancreas sections, cell counting rather than area measurement was performed by the Openlab software.

**Acknowledgements**

*We thank A. Efstratiadis for Igf1r*$^{+/-}$ *mice; B. Cheatham for anti-IRβ antibodies; and J. Marron for assistance in preparation of this manuscript. This work was supported by DK43808. D.J.W. is an MRC (UK) Clinician Scientist and D.J.B. was supported by a grant from the JDFI during a portion of these studies.*

Received 8 April; accepted 9 July 1999.

© 1999 Nature America Inc. • http://genetics.nature.com

© 1999 Nature America Inc. • http://genetics.nature.com


1. Cheatham, B. & Kahn, C.R. Insulin action and the insulin signaling network. *Endocr. Rev.* **16**, 117–142 (1995).
2. LeRoith, D., Werner, H., Beitner-Johnson, D. & Roberts, C. Molecular and cellular aspects of the insulin-like growth factor I receptor. *Endocr. Rev.* **16**, 143–163 (1995).
3. Baserga, R., Hongo, A., Rubini, M., Prisco, M. & Valentinis, B. The IGF-I receptor in cell growth, transformation, and apoptosis. *Biochem. Biophys. Acta* **1332**, F105–F126(1997).
4. Baserga, R. Oncogenes and the strategy of growth factors. *Cell* **79**, 927–930 (1994).
5. White, M.F. & Kahn, C.R. The insulin signaling system. *J. Biol. Chem.* **269**, 1–4 (1994).
6. Myers, M.G. Jr *et al*. IRS-1 is a common element in insulin and insulin-like growth factor-I signaling to the phosphatidylinositol3´-kinase. *Endocrinology* **132**, 1421–1430 (1993).
7. Liu, J.P., Baker, J., Perkins, J.A., Robertson, E.J. & Efstratiadis, A. Mice carrying null mutations of the genes encoding insulin-like growth factor I (Igf-1) and type 1 IGF receptor (Igf1r). *Cell* **75**, 59–72 (1993).
8. Accili, D. *et al*. Early neonatal death in mice homozygous for a null allele of the insulin receptor gene. *Nature Genet.* **12**, 106–109 (1996).
9. Kulkarni, R.N. *et al*. Tissue-specific knockout of the insulin receptor in pancreatic β cells creates an insulin secretory defect similar to that in type 2 diabetes. *Cell* **96**, 329–339 (1999).
10. Sun, X.J. *et al*. The expression and function of IRS-1 in insulin signal transmission. *J. Biol. Chem.* **267**, 22662–22672 (1992).
11. Sun, X.J. *et al*. Role of IRS-2 in insulin and cytokine signaling. *Nature* **377**, 173–177 (1995).
12. Bernal, D. *et al.* Amino acid polymorphisms are not associated with random type 2 diabetes among Caucasians. *Diabetes* **47**, 976–979 (1998).
13. Withers, D.J. *et al*. Disruption of IRS-2 causes type 2 diabetes in mice. *Nature* **391**, 900–903 (1998).
14. Araki, E. *et al*. Alternative pathway of insulin signalling in mice with targetted disruption of the IRS-1 gene. *Nature* **372**, 186–190 (1994).
15. Yamauchi, T. *et al*. Insulin signaling and insulin actions in the muscles and livers of insulin-resistant, insulin receptor substrate 1-deficient mice. *Mol. Cell. Biol.* **16**, 3074–3084 (1996).
16. Tamemoto, H. *et al*. Insulin resistance and growth retardation in mice lacking insulin receptor substrate-1. *Nature* **372**, 182–186 (1994).
17. Herrera, P.L. *et al*. Embryogenesis of the murine endocrine pancreas; early expression of pancreatic polypeptide gene. *Development* **113**, 1257–1265 (1991).
18. LeRoith, D., Parrizas, M. & Blakesley, V.A. The insulin-like growth factor-I receptor and apoptosis. Implications for the aging process. *Endocrine* **7**, 103–105 (1997).
19. Yenush, L., Zanella, C., Uchida, T., Bernal, D. & White, M.F. The pleckstrin homology and phosphotyrosine binding domains of insulin receptor substrate 1 mediate inhibition of apoptosis by insulin. *Mol. Cell. Biol.* **18**, 6784–6794 (1998).
20. Scaglia, L., Smith, F.E. & Bonner-Weir, S. Apoptosis contributes to the involution of β cell mass in the post partum rat pancreas. *Endocrinology* **136**, 5461–5468 (1995).
21. Scaglia, L., Cahill, C.J., Finegood, D.T. & Bonner-Weir, S. Apoptosis participates in the remodeling of the endocrine pancreas in the neonatal rat. *Endocrinology* **138**, 1736–1741 (1997).
22. Datta, S.R. *et al.* Akt phosphorylation of BAD couples survival signals to the cell-intrinsic death machinery. *Cell* **91**, 231–241 (1997).
23. Bruning, J.C., Winnay, J., Cheatham, B. & Kahn, C.R. Differential signaling by insulin receptor substrate 1 (IRS-1) and IRS-2 in IRS-1 deficient cells. *Mol. Cell. Biol.* **17**, 1513–1521 (1997).
24. Rother, K.I. *et al*. Evidence that IRS-2 phosphorylation is required for insulin action in hepatocytes. *J. Biol. Chem.* **273**, 17491–17497 (1998).
25. Velloso, L.A., Carneiro, E.M., Crepaldi, S.C., Boschero, A.C. & Saad, M.J. Glucose- and insulin-induced phosphorylation of the insulin receptor and its primary substrates IRS-1 and IRS-2 in rat pancreatic islets. *Growth Regul.* **377**, 353–357 (1995).
26. Schuppin, G.T. *et al*. A specific increased expression of insulin receptor substrate 2 in pancreatic β-cell lines is involved with mediating serum-stimulated β-cell growth. *Diabetes* **47**, 1074–1085 (1998).
27. Hugl, S.R., White, M.F. & Rhodes, C.J. IGF-1 stimulated pancreatic β-cell growth is glucose dependent: synergistic activation of IRS-mediated signal transduction pathways by glucose and IGF-1 in INS-1 cells. *J. Biol. Chem.* **273**, 17771–17779 (1998).
28. Sawka-Verhelle, D. *et al*. Tyr624 and Tyr628 in insulin receptor substrate-2 mediate its association with the insulin receptor. *J. Biol. Chem.* **272**, 16414–16420 (1997).
29. Sawka-Verhelle, D., Tartare-Deckert, S., White, M.F. & Van Obberghen, E. Insulin receptor substrate-2 binds to the insulin receptor through its phosphotyrosine-binding domain and through a newly identified domain comprising amino acids 591–786. *J. Biol. Chem.* **271**, 5980–5983 (1996).
30. Vaisse, C., Kim, J., Espinosa, R. III, Lebeau, M.M. & Stoffel, M. Pancreatic islet expression studies and polymorphic DNA markers in the genes encoding hepatocyte nuclear factor-3α, -3β, -3γ, -4γ, and -6. *Diabetes* **48**, 1364–1367 (1997).
31. Ahlgren, U., Jonsson, J., Jonsson, L., Simu, K. & Edlund, H. β-cell-specific inactivation of the mouse Ipf1/Pdx1 gene results in loss of the β-cell phenotype and maturity onset diabetes. *Genes Dev.* **12**, 1763–1768 (1998).
32. Edlund, H. Transcribing pancreas. *Diabetes* **47**, 1817–1823 (1998).
33. Sharma, S. *et al*. Hormonal regulation of an islet-specific enhancer in the pancreatic homeobox gene STF-1. *Mol. Cell. Biol.* **17**, 2598–2604 (1997).
34. Guz, Y. *et al*. Expression of murine STF-1, a putative insulin gene transcription factor, in β cells of pancreas, duodenal epithelium and pancreatic exocrine and endocrine progenitors during ontogeny. *Development* **121**, 11–18 (1995).
35. Baker, J., Liu, J.P., Robertson, E.J. & Efstratiadis, A. Role of insulin-like growth factors in embryonic and postnatal growth. *Cell* **75**, 73–82 (1993).
36. Swenne, I. Pancreatic β-cell growth and diabetes mellitus. *Diabetologia* **35**, 193–201 (1992).


© 1999 Nature America Inc. • http://genetics.nature.com